Faraday Discuss., 1994, **97**, 43–55

Is the NH_3–NH_3 Riddle solved?

Ad van der Avoird, Edgar H. T. Olthof and Paul E. S. Wormer
Institute of Theoretical Chemistry, University of Nijmegen Toernooiveld, 6525 ED Nijmegen, The Netherlands

Vibration–rotation–tunnelling (VRT) splittings have been computed for the dimer $(NH_3)_2$ by the use of four different model potentials, which have different barriers to internal rotations and to the interchange of the donor and the acceptor in the hydrogen bond. The six-dimensional nuclear motion problem is solved variationally for $J = 0$ and $J = 1$ in a symmetry adapted basis consisting of analytic radial functions and rigid rotor functions depending on the five internal angles. Dipole moments, nuclear quadrupole splittings and the amount of quenching of the monomer umbrella inversions are also computed. Good agreement with the experimental data available for $(NH_3)_2$ is obtained for a potential that has an equilibrium hydrogen-bonded structure close to linear, but a low interchange barrier (24 cm^{-1}). Although even the mixed *ortho–para* states have large amplitude motions with this potential, our calculations on $(ND_3)_2$ still explain the near absence of shifts in the nuclear quadrupole splittings and the observed change in the dipole moment upon isotope substitution.

Especially since the finding of the 'surprising', nearly cyclic, structure by Nelson *et al.*[1] in 1985, the question of whether $(NH_3)_2$ is hydrogen bonded has occupied many theorists and experimentalists. Most *ab initio* calculations[2,3] led to a classical, nearly linear, hydrogen-bonded structure. The calculations by Sagarik *et al.*[4] seemed to support the nearly cyclic structure, but it was convincingly argued later[5] that a slight bending of the linear hydrogen bond in these calculations would have favoured the classical hydrogen-bonded structure. In fact, it was shown in ref. 6 that the analytical model potential which Sagarik *et al.* fitted to their *ab initio* data indeed supports a slightly bent hydrogen-bonded structure as the most stable one. The two most recent, and most sophisticated, calculations differ in the prediction of the equilibrium structure: Hassett *et al.*[5] predicted a hydrogen-bonded structure, whereas Tao and Klemperer[7] predicted a cyclic structure thanks to the addition of bond functions.

An obvious explanation of the discrepancy between the outcome of most calculations and the microwave data which led Nelson *et al.*[1] to their 'surprising structure' might be found in the effect of vibrational averaging: whereas the electronic structure calculations focus mainly on finding the minimum of the intermolecular potential, the experiment gives a vibrationally averaged structure. This question was addressed experimentally by Nelson *et al.*[8,9] by means of various isotope substitutions. From the fact that the relevant intermolecular bond angles hardly change with isotope substitution they conclude that $(NH_3)_2$ is fairly rigid and that its equilibrium structure must be (nearly) cyclic. They supported this latter conclusion by the observation that the dipole moment of $(ND_3)_2$, in which the vibrational averaging effects are expected to be less

than in $(NH_3)_2$, is even smaller (it is 0.57 D)† than the already small value of 0.74 D which indicated the occurrence of the nearly cyclic structure in $(NH_3)_2$.

The effects of vibrational averaging have been assessed theoretically by van Bladel *et al.*[6] Using the model potential of Sagarik *et al.*,[4] which was the only full potential surface available from *ab initio* calculations, the six-dimensional Schrödinger equation for the intermolecular (or Van der Waals) motions was solved, in a basis of (coupled) internal rotor functions and Morse-type stretch functions. Although we found that the vibrationally averaged structure was shifted from the equilibrium hydrogen-bonded structure toward the cyclic geometry, we were not able to obtain complete reconciliation with the microwave geometry. Since our potential was not very reliable, our results were not conclusive, although they did show that the dimer is floppy and that accordingly the effect of vibrational averaging is very important, not only for the geometry, but also for other measured properties such as the dipole moment and nuclear quadrupole splittings. Further, we obtained indirect evidence that the umbrella inversion of the two monomers is not completely quenched, as was assumed by Nelson *et al.*[1]

The latter conclusion was also reached by Loeser *et al.*,[10] who reported an extensive set of new far-infrared (FIR) and microwave measurements and gave a very detailed analysis of these, as well as previous,[11] experimental data. They conclude that the group of feasible operations (permutations, inversion and their products) is of order 144, which implies that they observed the tunnelling splittings associated with the two umbrella inversions and the interchange tunnelling in which the role of the two monomers is reversed. The same conclusion was reached by Havenith *et al.*,[12] on the basis of IR/FIR double-resonance experiments. The latter authors also measured the dipole moment in the $|K| = 1$ state of G-symmetry.[13] We predicted earlier[6] that the $|K| \geqslant 1$ states of E_3 and E_4 symmetry have non-vanishing dipole moments too. Measurements to verify this prediction were recently performed in Nijmegen, but since the hyperfine pattern in an electric field is complicated, the analysis of these measurements is still in progress.

Thus, the various experimental approaches present (seemingly) conflicting evidence regarding the rigidity of $(NH_3)_2$ and its equilibrium structure. Also the different *ab initio* calculations lead to different pictures. Multiple discussions[9,14,15] have been devoted to this riddle. In this paper we present a new, and more complete, theoretical approach. We have constructed four different model potentials with different barriers in the interchange motion and in the hindered rotations of the two NH_3 monomers around their C_3 axes. For each of these potentials we have calculated the six-dimensional VRT states and the various transition frequencies which have been observed. For various states we have also computed the expectation values of the dipole moment and the nuclear quadrupole splittings, which are indicative of the orientations of the NH_3 monomers in the complex. Furthermore, we have explicitly evaluated the tunnelling frequencies associated with the hindered NH_3 umbrella inversions. All these data have been compared with the corresponding experimental values now available.[1,8,10–13] From this comparison we have concluded already[16] that one of our model potentials must be fairly close to the actual NH_3–NH_3 potential. The equilibrium goemetry in this potential is a nearly linear hydrogen-bonded structure with a dipole moment of 1.42 D. In the present work we have used this potential, as well as the other model potentials, to calculate the VRT states of ND_3–ND_3 and the corresponding dipole moments and nuclear quadrupole splittings. We study, in particular, whether the observed effects of isotope substitution on the dipole moment and on the (average) monomer orientations can be reproduced. Since our favoured potential has an interchange barrier of only 24 cm^{-1}, we discuss how the observed (small) effects of isotope substitution can be explained also on the basis of a highly non-rigid dimer structure.

† 1 D $\approx 3.335\,64 \times 10^{-30}$ C m.

Model Potentials and the Calculation of the Vibration–Rotation–Tunnelling States

All our present potentials use the permanent multipole moments (calculated[17] at the MP2 level) on the NH_3 monomers to model the electrostatic interactions, in combination with an exp-6 site–site potential

$$V_{AB} = \sum_{i \in A} \sum_{j \in B} \left[A_i A_j \exp[-(b_i + b_j)R_{ij}] - \frac{c_i c_j}{R_{ij}^6} \right] \quad (1)$$

for the exchange repulsion and dispersion interactions. By changing the parameters A_i in the exchange repulsion we are able to alter the shape of the potential surface and, in particular, to vary the barriers to internal rotation and to interchange of the monomers. Since induction effects are not explicitly included and we will finally 'optimize' the potential surface by comparison with the experimental data, our potentials must be considered as largely empirical. In potentials I and II we have merely included the electrostatic interactions between the dipole and quadrupole moments of NH_3, just as Dykstra and Andrews[18] did in their model potential. In potentials III and IV we have added the octupole moments. This is essential, as discussed below, because the dipole and quadrupole of NH_3 have only axial components and the octupole yields the first contributions to the electrostatic interactions that depend on the directions of the individual N—H bonds. Following the work of Dykstra and Andrews,[18] we considered, in addition to the nitrogen nuclei and protons, the nitrogen lone pairs as centres of force. See Table 1 for the locations of these centres and Table 2 for different sets of force field

Table 1 Ammonia structure[a]

r_{HC}	0.988 51 Å
r_{HN}	1.012 00 Å
r_{NC}	0.067 66 Å
r_{LN}	0.988 51 Å

[a] C is centre of mass. L is lone pair force centre.

Table 2 Potentials/au[a]

	I	II	III	IV
Q_0^1	−0.6106	−0.6106	−0.6106	−0.6106
Q_0^2	−2.1598	−2.1598	−2.1598	−2.1598
Q_0^3	0.0	0.0	2.5226	2.5226
Q_3^3	0.0	0.0	4.1748	4.1748
c_N	14.0	14.0	14.0	14.0
c_L	0.0	0.0	0.0	0.0
c_H	0.2	0.2	0.2	0.2
b_N	1.8391	1.8391	1.8391	1.8391
b_L	1.5549	1.5549	1.5549	1.5549
b_H	1.5549	1.5549	1.5549	1.5549
A_N	207	207	280	255
A_L	9.336 (−4)	8.000 (−3)	5.000 (−4)	2.000 (−3)
A_H	1.541 (−2)	4.880 (−2)	1.000 (−2)	1.540 (−2)

[a] 1 au of energy $= E_h = 4.359748 \times 10^{-18}$ J, 1 au of charge = e = 1.602177×10^{-19} C, 1 au of length $= a_0 = 0.529177 \times 10^{-20}$ m. Electric moments from ref. 17, for the other parameters see text.

parameters used in this work. The parameters c_i were taken from Dykstra *et al.* The parameters A_i and b_i in potential I were determined from the (6–12) Lennard-Jones (LJ) potential of Dykstra *et al.* by requiring that the depth and the position of the minimum in the N–N and H–H terms of eqn. (1) coincide with the minimum in the corresponding term of the LJ potential. The reason why we did not use the LJ potential itself was the following. Our dynamics program requires the potential as a linear combination of angular functions, so that we always expand our model potentials. We experienced convergence problems when we tried to expand the (6–12) LJ potential. Switching to the exp-6 potential solved this problem. Since the Dykstra potential does not contain octupoles, we obtain too much attraction when adding octupoles (potentials III and IV), which we compensated for by increasing the parameter A_N. Since the nitrogen atoms almost coincide with the respective centres of mass, this hardly affects the anisotropy in the interaction.

Potential I, which by design resembles the Dykstra potential, has an interchange barrier of 31.1 cm^{-1}. By increasing A_L and A_H we obtained potential II. As an increase of these parameters lowers the barrier, we could achieve a minimum in potential II at about the position of the saddle point of I. Thus potential II was designed to have its minimum for a cyclic structure. Potential III corresponds to I with an octupole added and IV resembles potential II in its interchange behaviour, but differs by the presence of an octupole.

In view of the origin of hydrogen bonding it is interesting to consider the role of the electrostatic interactions. If we fix the distance at $R = 3.23$ Å (which is close to the observed equilibrium distance) and switch on just the dipole and quadrupole interactions, we find a minimum in the potential for $\theta_A = 18°$ and $180° - \theta_B = 100°$ (the angles are defined in Fig. 1). These are the angles expected in a hydrogen-bonded structure. Note, however, that the energy in this simple model does not depend on ϕ_A or ϕ_B, because the dipole and the quadrupole tensor are axial and the positions of the protons of monomer B are undetermined with respect to the lone pair of monomer A. When the octupoles are added, monomer B rotates around its three-fold axis such that one of its protons is close to the lone pair of A. The minimum structure is at $(\theta_A, 180° - \theta_B) = (20°, 99°)$ and $(\phi_A, \phi_B) = (60°, 0°)$, with R still fixed at 3.23 Å. Thus, this simple electro-

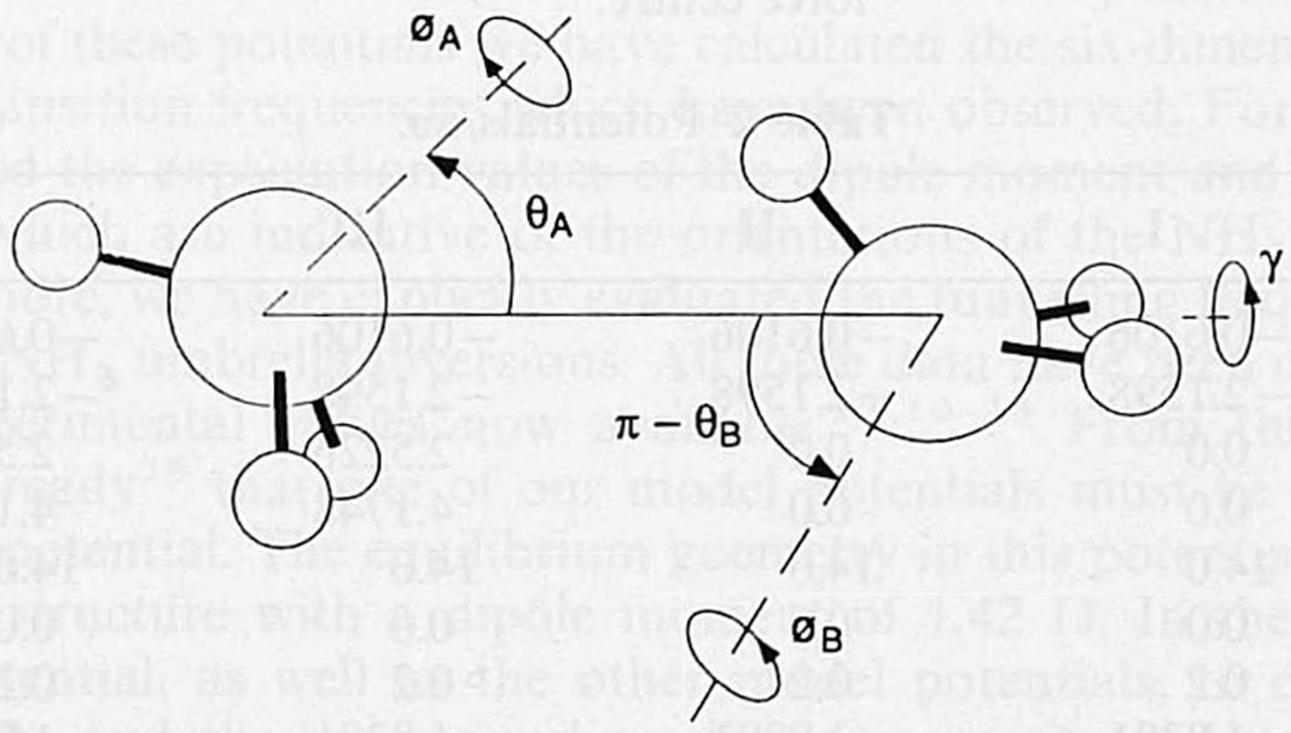

Fig. 1 The relevant coordinates of the dimer. The angles are defined as follows: We take two parallel frames centred on A and B and let the postive z-axes point from the centre of mass of A to that of B. The plane of the drawing coincides with the xz-planes with the x-axes pointing upward. Consider a geometry with two parallel umbrellas, the symmetry axes on the z-axes and the plane of paper as a symmetry plane. Each monomer has an N—H bond in its xz-plane with positive x-coordinate and negative z. This is the geometry with all angles zero. Next we rotate the symmetry axes such that they have polar angles θ_X, γ_X, where X = A, B. Then $\gamma = \gamma_B - \gamma_A$. Finally we rotate the monomers around their symmetry axes over angles ϕ_A and ϕ_B, respectively. A positive rotation is in the direction of the lone pair.

static model predicts already the classical hydrogen-bonded structure with its characteristic well directed bond. When we vary simultaneously (θ_A, $180° - \theta_B$) from the one minimum at (20°, 99°) to the other equivalent minimum at (81°, 160°), while minimizing the energy by relaxing the angles γ, ϕ_A and ϕ_B, we walk over the interchange tunnelling path. The barrier that is herewith crossed has height 126.8 cm^{-1} on the dipole–quadrupole–octupole surface, see Fig. 2(*a*), where we exhibit the energy as a function of θ_A and θ_B. Note that electrostatics allows interchange tunnelling only through a narrow valley.

When we add the exp-6 terms to the electrostatic potential, the interchange tunnelling path still runs through this valley, see Fig. 2(*b*). The height of the barrier of this valley is affected by the repulsions, however, especially those between the proton of monomer **B** that takes part in the hydrogen bond and the lone pair of monomer **A**. By increasing this repulsion both monomers are rotated toward a cyclic structure (a simultaneous increase of θ_A and θ_B) and the interchange barrier is lowered. In potentials I and III we have maintained a barrier of about 25 cm^{-1}, in potentials II and IV the barriers have practically vanished. The ϕ_A and ϕ_B dependence of I *versus* III and II *versus* IV are completely different, of course, because of the octupoles. In Table 3 we have listed some characteristic data of all four potentials. Notice, parenthetically, that we present values of $180° - \theta_B$ in Table 3, rather than of θ_B, because whenever $\theta_A \approx 180° - \theta_B$, we have a cyclic structure.

In Fig. 3 the energy on the interchange path for the four different potentials is shown together with the potential of Sagarik *et al.*[4] that we used in our earlier VRT calculations.[6] Note that this potential has the highest barrier (83.5 cm^{-1}), whereas potential I has only 31.1 cm^{-1} in close agreement with the *ab initio* barrier of Hassett *et al.*,[5] who find 29.3 cm^{-1}. Potential III has the even lower barrier height of 24.4 cm^{-1}. Hassett *et al.* find their minimum at $(\phi_A, \phi_B) = (60°, 0°)$. Note from Table 3 that our potentials without octupoles yield minima for $(\phi_A, \phi_B) = (0°, 60°)$, and that potentials III and IV agree with Hassett *et al.* in the minimum ϕ-values. The recent potential by Tao and Klemperer[7] resembles in its θ-dependence potentials II and IV, which favour a cyclic structure.

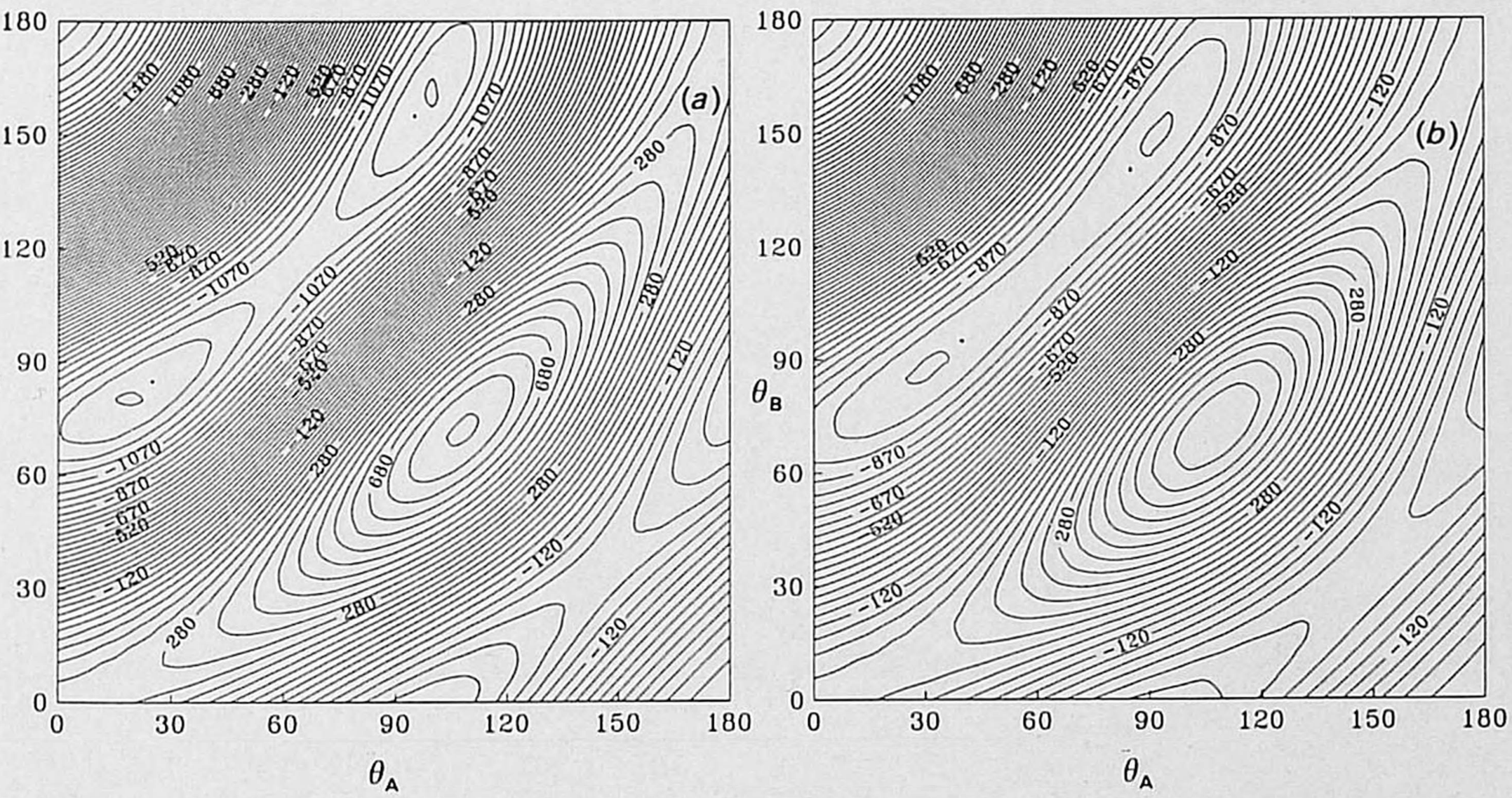

Fig. 2 Potential III (in cm^{-1}) as a function of θ_A and θ_B, with ϕ_A, ϕ_B and γ fixed at their equilibrium values (60°, 0° 180°). (*a*) Electrostatic dipole–quadrupole–octupole interaction energy at $R = 3.23$ Å. (*b*) Total potential III, with $R = 3.373$ Å; observe the same valley for interchange tunnelling as in the purely electrostatic case of (*a*).

Table 3 Equilibrium coordinates and barrier heights in different potentials[a]

	I	II	III	IV[b]
R	3.236	3.296	3.366	3.330
θ_A	29.8	62.6	32.0	49.5
$180° - \theta_B$	92.0	62.6	91.5	76.3
ϕ_A	0.0	0.0	60.0	60.0
ϕ_B	60.0	60.0	0.0	0.0
μ_e[c]	1.49	0.00	1.42	0.67
ΔE_{AB}[d]	31.1	0.0	24.4	1.0
	(23.7)	(0.0)	(25.2)	(0.0)
ΔE_A[e]	2.2	32.7	26.7	80.9
ΔE_B[e]	159.6	32.7	335.4	258.5

[a] Distances in Å, angles in degrees, energies in cm^{-1}. [b] Although the equilibrium geometry in potential IV does not correspond to a cyclic structure, this potential is flat along the interchange tunnelling path and its shape is almost equal to that of II, see Fig. 3. [c] μ_e/D is the dipole moment at the equilibrium geometry. [d] ΔE_{AB} is the height of the saddle point in the $\theta_A\,\theta_B$-plane (other coordinates relaxed); the values in brackets are from the expanded potential. [e] ΔE_X is the barrier crossed in varying ϕ_X, X = A, B (other coordinates at their equilibrium values).

Before we actually use these potentials to calculate the VRT states we expand them in a complete set of angular functions (coupled products of Wigner D-functions depending on the orientations of both monomers). The procedure to perform this expansion is extensively described in ref. 6 and 16. Note that we have carefully checked that the

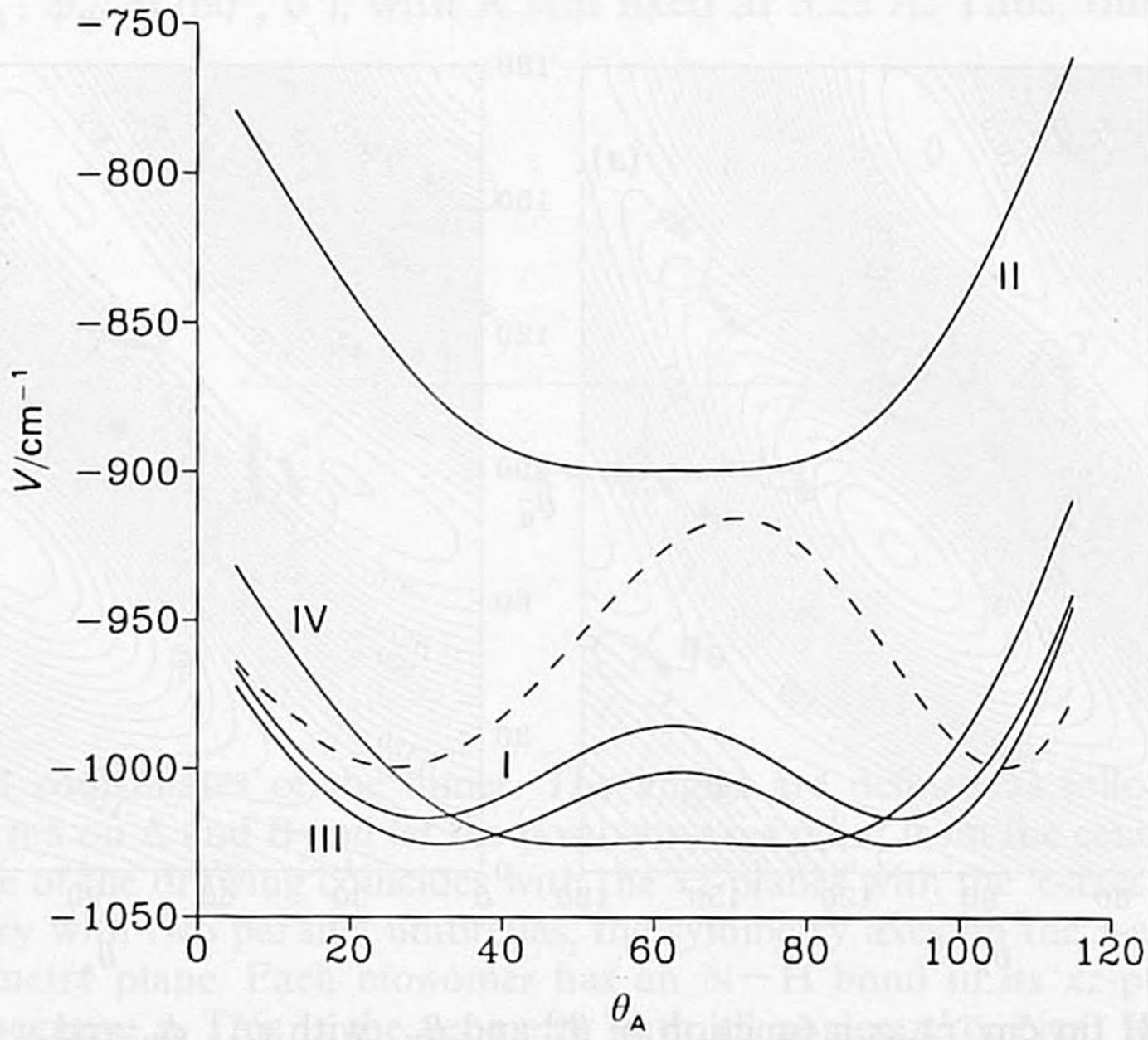

Fig. 3 The energy on the interchange path for four different model potentials, *cf.* Table 3, indicated by full lines. The dashed line is the potential of Sagarik *et al.*[4] θ_A is varied, the other coordinates are relaxed, so as to minimize the interaction energy.

truncation of these expansions at $L_A^{max} = L_B^{max} = 5$ does not significantly affect the shape of the potential surfaces. In Table 3 we show this by giving also the heights of the interchange barriers in the expanded potentials; this is an important and sensitive quantity.

The Hamiltonian that has to be diagonalized in order to obtain the VRT states is given in ref. 6, 16 and 19. The basis and the calculation of the matrix elements are described in these references. In most calculations we have truncated the basis at $j_A^{max} = j_B^{max} = 5$, but, as shown below, in various critical cases it has been checked by increasing $j_A^{max} = j_B^{max}$ to 6 that our conclusions are not affected by the limited size of the basis. The rotational constants of NH_3 were taken as $A_x = A_y = 9.945\ cm^{-1}$ and $A_z = 6.229\ cm^{-1}$, those[20] of ND_3 as $A_x = A_y = 5.143\ cm^{-1}$ and $A_z = 3.124\ cm^{-1}$, the masses as $m_H = 1.0078$ u,† $m_D = 2.0140$ u and $m_N = 14.0031$ u.

In the calculations on $(ND_3)_2$ we would have to transform the potentials from the coordinates of Fig. 1, to a set of similar coordinates which are defined with respect to the ND_3 centres of mass. For the site–site contribution to the potentials this transformation is trivial. It is also easy to re-express the NH_3 multipole moments with respect to the ND_3 mass centre, but the truncated multipole–multipole interaction series is not invariant under the centre of mass translations. In fact, we found that the truncation error, which affects the well depth and the barrier heights, is considerably larger than the error which is made by using the $(NH_3)_2$ potentials for $(ND_3)_2$ without transformation, which just affects the coordinates. Since the centres of mass shift by 0.047 Å, with a distance $R \approx 3$ Å the corresponding changes in the angles θ_A, θ_B, *etc.*, are only about one degree. Hence, we decided to use the $(NH_3)_2$ potentials directly for $(ND_3)_2$ and to study the isotope effects by just changing the masses and the rotational constants of the monomers. Actually, this choice shows the isotope effects in their purest form. We will have to ensure, however, that the quantitative results are not significantly affected by this hypothesis.

It was essential to use the full symmetry of the system in our calculations. The molecular symmetry group, which by definition consists of feasible permutations and inversion, is of order 36 provided we assume the umbrella inversions to be frozen. Otherwise it is of order 144. These groups are denoted as G_{36} and G_{144}, respectively. In this work we will mainly focus on G_{36}, which has four one-dimensional irreducible representations (irreps), designated A_i, $i = 1, \ldots, 4$, four two-dimensional irreps (E_i, $i = 1, \ldots 4$) and one four-dimensional irrep G. The sets of A_i symmetry (A_i) are states of two *ortho* monomers, those of E_i symmetry (E_i) belong to two *para* monomers and G sets describe a mixed *ortho–para* dimer. For more details on the symmetry adaptation of our basis see the Appendix of ref. 6.

Results

$(NH_3)_2$

The results from our calculations on $(NH_3)_2$ are summarized in Tables 4 and 5, for $K = 0$ and $|K| = 1$, respectively. Note that K, which is the projection of the total angular momentum J on the dimer bond axis, is not an exact quantum number. Since the off-diagonal Coriolis coupling is small, however, the observed states can be well characterized by K and we could neglect this coupling in our calculations. The energy differences $E_{A_4} - E_{A_1}$ and $E_{E_2} - E_{E_1}$ in Table 4 are due to the interchange tunnelling. Note that these differences are large, of the order of 20 cm^{-1}, which confirms that the interchange between the donor and the acceptor molecule in the hydrogen bond takes place rapidly. Also the splitting $E'_G - E_G$ between the lowest G states is partly due to

† 1 u $\approx 1.660\,540 \times 10^{-27}$ kg.

Table 4 Comparison of computed and measured quantities for NH_3–NH_3; all quantities pertain to $K = 0$

	calc. potentials				
	I	II	III	IV	expt.
dipole[a]	−0.69	−0.32	−0.92	−0.53	0.74
$\langle\theta_A\rangle_G$[b]	46°	53°	44°	51°	49°
$\langle 180° - \theta_B\rangle_G$[b]	63°	62°	66°	64°	65°
$E_{A_4} - E_{A_1}$[c]	587	1027	509	779	483
$E_{E_2} - E_{E_1}$[c]	535	825	603	886	577
$E'_G - E_{G_2}$[c]	637	965	680	879	614
$E_{G_2^-} - E_{G_2^+}$[c]	2.49	1.19	3.12	1.89	3.31
$E'_{G_2^-} - E'_{G_2^+}$[c]	1.40	0.82	1.21	1.76	2.39

[a] In D; at the G ground state. With the (larger) basis truncated at $j_A^{max} = j_B^{max} = 6$ the value calculated from potential III is −0.94 D. The sign is undetermined experimentally. [b] From $\langle P_2(\cos\theta)\rangle$; G ground state. [c] Energy differences in GHz, 1 GHz = 0.03336 cm^{-1}.

this interchange tunnelling, but partly due, as well, to the difference between the *ortho* and the *para* monomers that form these G states. It is typical that the G states are more or less localized on one side of the interchange barrier, see Fig. 4(*a*), in contrast with the A_i and E_i states, which are either symmetric or antisymmetric with respect to interchange. Even for the potentials II and IV with no interchange barrier the G states are non-cyclic and possess a (small) dipole moment, see Table 4.

Another important observation is that the actual difference between the *ortho* and *para* monomers, which manifests itself in the G state expectation values of the dipole moment, can be influenced by changing the barriers to rotation over ϕ_A and ϕ_B. So, potentials III and IV which have substantially larger ϕ_A and ϕ_B barriers (see Table 3), due to the monomer octupole moments, lead to larger dipole moments than potentials I

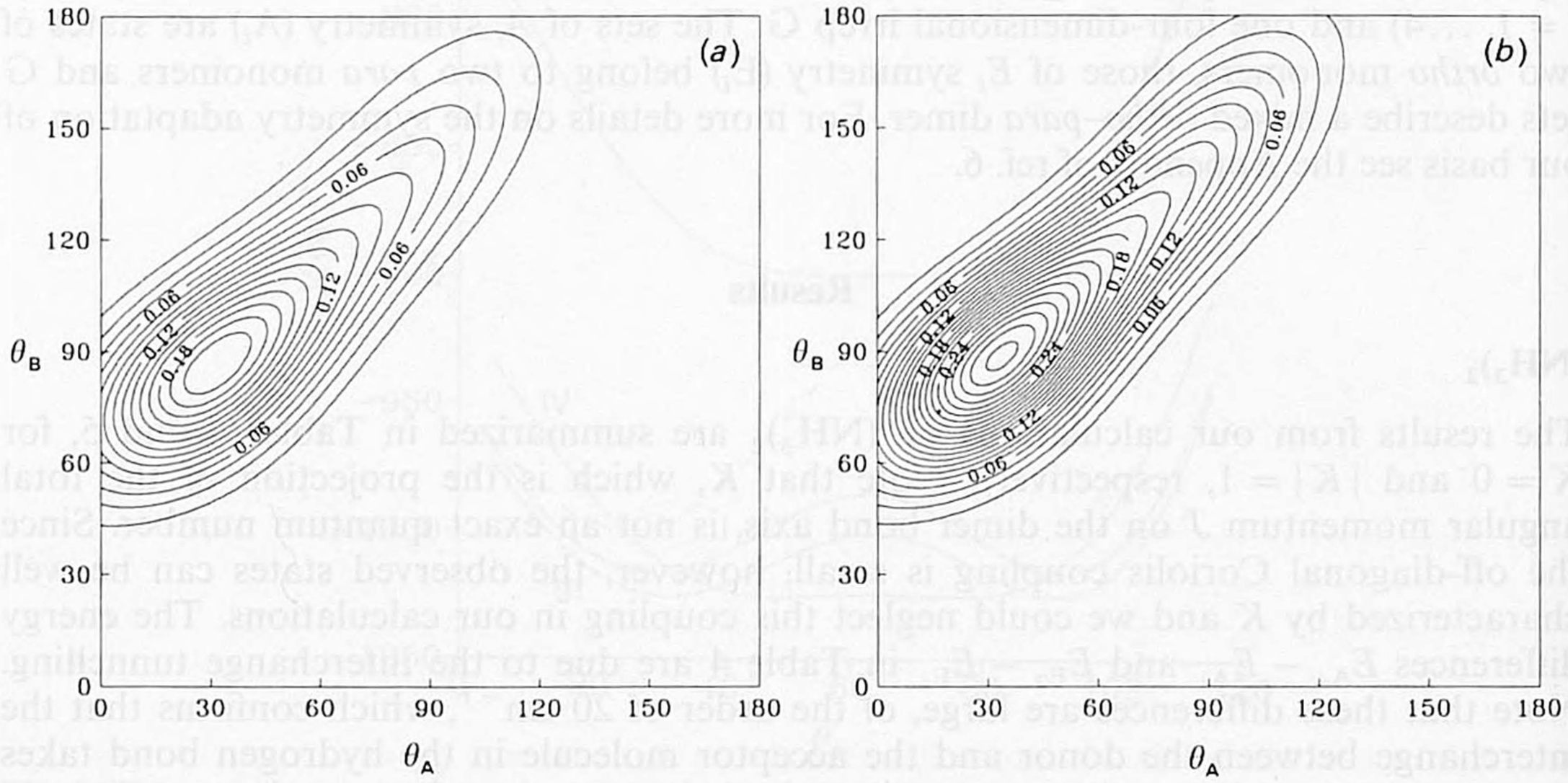

Fig. 4 The lowest *G*-state wavefunctions (absolute squared) of (*a*) NH_3–NH_3 and (*b*) ND_3–ND_3 in the θ_A–θ_B plane. Potential used: III. ϕ_A, ϕ_B and γ are fixed at their equilibrium values (60°, 0°, 180°) and R = 3.373 Å.

and II, in spite of the similarity between the potentials I and III and between II and IV along the interchange path (see Fig. 3).

The final two splittings in Table 4 are due to monomer umbrella inversion. An exact calculation requires the solution of an eight-dimensional dynamics problem: the six coordinates of Fig. 1 plus the two umbrella angles ρ_A and ρ_B. The group of this system is G_{144} and the labels $G_2^{\pm}$ refer to irreps of this group. These irreps correlate with the irrep G of $G_{36} \subset G_{144}$. A dynamics problem of this size cannot be handled at present, so that we had to resort to a simple model which is an extension of a model we proposed earlier for Ar–NH_3.[21] Briefly, the model entails the computation of the expectation value of the inversion parts of the monomer Hamiltonians, $H_{inv}(\rho_A) + H_{inv}(\rho_B)$, with respect to the functions $[E - (56)][E \mp (56)^*]\Psi_{vdw} f(\rho_A) f(\rho_B)$, where $(56)^*$ is the operator inverting monomer A and (56) inverts B. The wavefunction Ψ_{vdw} is the lowest, or the one but lowest, eigenstate of H_{vdw} of G symmetry, $f(\rho_A)$ and $f(\rho_B)$ are ground umbrella (v_2) states of A and B localized in one of the wells of their respective monomers. Assuming that $\langle f(\rho_A) | (56)^* | f(\rho_A) \rangle = 0$ and an equivalent relation on B, we obtain for the splitting

$$E_{G_2^-} - E_{G_2^+} = \Delta \langle \Psi_{vdw} | (56)^* | \Psi_{vdw} \rangle \tag{2}$$

where $\Delta = 0.793\ cm^{-1}$, the tunnelling splitting of the free monomer.[22] This splitting corresponds to the inversion of the *para* partner in the dimer. In a forthcoming paper[23] we will present more details on this model and its group theoretical implications.

Let us now focus on the comparison with the experimental data for $(NH_3)_2$. First of all, let us mention that the four model potentials introduced here, which all have interchange barriers between 0 and 30 cm^{-1}, yield substantially better agreement with the microwave and FIR spectra than the potential that we used earlier,[6] which has a barrier of about 80 cm^{-1}. In particular, potentials I and III which have barriers of about 25 cm^{-1} give good interchange tunnelling splittings $E_{A_4} - E_{A_1}$, $E_{E_2} - E_{E_1}$, and $E'_G - E_G$ (see Tables 4 and 5). The splittings obtained from potentials II and IV, which have practically no barriers, are substantially too high. The angles θ_A and θ_B that correspond to the nuclear quadrupole splittings are fairly close to the experimental values[1] for all the model potentials, much closer than the results in our earlier paper.[6] The best dipole moment, measured for the ground state of G symmetry just as the quadrupole splittings, is obtained from potential I. The other potential that yields realistic interchange tunnelling splittings, potential III, gives a dipole moment which is just slightly too large. Note that the dipole moment is 2.29 D in the nearly linear hydrogen-bonded structure that corresponds to the equilibrium structure of the potential in ref. 6, while the average dipole in that paper is 1.60 D. Even for potential I with its good average dipole moment

Table 5 Energy splittings and dipoles of NH_3–NH_3 for the lowest G states with $|K| = 1$

	calc. potentials				
	I	II	III	IV	expt.
$E_1 - E_0$[a]	256	226	186	169	118[c]
$E_2 - E_0$[a]	582	970	484	741	486[c]
$E_3 - E_0$[a]	978	1103	976	1160	865[c]
$\langle\mu\rangle_0$[b]	0.31	0.057	−0.13	−0.046	0.10[d]
$\langle\mu\rangle_1$[b]	−0.96	−0.44	−0.85	−0.50	—
$\langle\mu\rangle_2$[b]	−0.29	−0.033	0.12	0.029	<0.09[d]

[a] In GHz. [b] In D. [c] Ref. 10. [d] Ref. 13. The sign is undetermined experimentally.

of 0.69 D, the dipole that corresponds to the equilibrium geometry of the dimer is still 1.49 D. This is characteristic for the lack of rigidity of $(NH_3)_2$ along the interchange coordinate, as are the deviations between the average angles θ_A and θ_B obtained from the quadrupole splittings and the average angles that correspond to the dipole moment.

Yet another sign of this non-rigidity is the recent[13] finding that the dipole moment ($\mu = 0.10$ D) of the lowest G state with $|K| = 1$ is much smaller than the dipole ($\mu = 0.74$ D) of the G ground state with $K = 0$. This finding is qualitatively reproduced by all the present model potentials; potential III gives the best quantitative agreement ($|\mu| = 0.13$ D). Our calculations predict further that the first excited G state with $|K| = 1$ has a much larger dipole moment, which does not differ much from the ground state $K = 0$ value. It should be possible to check this prediction experimentally by the measurement of Stark splittings. Furthermore, we observe (see ref. 16) that the G levels with $|K| = 1$ are now correctly positioned, relative to the G levels with $K = 0$. In ref. 6 we still found the lowest G level with $|K| = 1$ to be below the lowest level with $K = 0$. Again, potential III gives the best agreement with the observed frequencies, see Table 5.

All the model potentials of the present paper yield quite realistic values for the umbrella inversion splittings. Remember that this splitting in the free NH_3 monomer amounts to 23 GHz. In the last two lines of Table 4 we see that in the dimer this tunnelling motion is about 10 times slower, which is correctly reflected by all the model potentials. Group theory shows (ref. 23) that the observed G-state splittings correspond with the inversion of the *para* monomer. Our calculations tell us that in the ground state of G symmetry (with $K = 0$) this is predominantly the proton donor, in the first excited G state with $K = 0$ it is the proton acceptor. Although, of course, the difference between the acceptor and the donor vanishes for the cyclic structure, it is still (slightly) present even when the potential has a cyclic equilibrium geometry, due to the inequivalence between the *ortho* and *para* monomers in the G states. So, the experimentally observed inversion splittings imply that the inversion of the proton donor is less hindered than the inversion of the acceptor, a fact which is correctly reflected by all the calculated results. From the wavefunctions obtained in ref. 6 we calculate inversion splittings of 1.67 GHz and 0.09 GHz, for the ground and first excited G state, respectively. As before, we find that the present potentials, which yield more nearly equivalent monomers, give far better results than the potential used in ref. 6.

Among these new potentials it is potential III that gives the best overall agreement with the, now rather extensive, set of spectroscopically observed properties of $(NH_3)_2$. At this stage of our investigations, we were very anxious to find out whether potential III would also reproduce the observed decrease of the G-state dipole moment when going from $(NH_3)_2$ to $(ND_3)_2$. Since the value of the dipole at the equilibrium geometry of potential III is 1.42 D, much larger than the average value of 0.92 D, and one would expect $(ND_3)_2$ to stay closer to equilibrium than $(NH_3)_2$, we did not expect to find this decrease in our calculations.

$(ND_3)_2$

The results from our calculations on $(ND_3)_2$ which are most relevant for comparison with the quantities observed by Nelson *et al.*[8] are collected in Table 6. First, we note that the interchange tunnelling frequencies, which have not been measured yet, are 20 to 30% smaller than in $(NH_3)_2$. This decrease is well in line with the ratio between the rotational constants: $(A_x^{ND_3}/A_x^{NH_3})^{1/2} = 0.72$. For the potentials II and IV we observe a substantial decrease of the average dipole moments, which, in view of the preference for the cyclic structure in these potentials, might be expected too. To us, it came as a surprise, however, that the average dipole moment also decreases for potential III, from 0.92 D for $(NH_3)_2$ to 0.74 D for $(ND_3)_2$. This decrease follows nicely the experimentally observed[8] decrease from 0.74 D for $(NH_3)_2$ to 0.57 D for $(ND_3)_2$. Also, the accompany-

Table 6 Comparison of computed and measured quantities for ND_3–ND_3; all quantities pertain to $K = 0$

	calc. potentials				
	I	II	III	IV	expt.
dipole[a]	−0.68	−0.24	−0.74	−0.34	0.57
$\langle\theta_A\rangle_G$[b]	46°	55°	46°	53°	50°
$\langle 180° - \theta_B\rangle_G$[b]	64°	62°	64°	62°	63°
$E_{A_4} - E_{A_1}$[c]	435	845	431	720	—
$E_{E_2} - E_{E_1}$[c]	370	657	518	824	—
$E'_G - E_G$[c]	456	785	519	767	—

[a] In D; G ground state. With the (larger) basis truncated at $j_A^{max} = j_B^{max} = 6$ the value calculated from potential III is −0.76 D. The sign is undetermined experimentally. [b] From $\langle P_2(\cos\theta)\rangle$; G ground state. [c] Energy differences in GHz.

ing changes in the angles θ_A and θ_B from the expectation values $\langle P_2(\cos\theta_A)\rangle$ and $\langle P_2(\cos\theta_B)\rangle$ agree well with the changes observed by measuring the nuclear quadrupole splittings in $(NH_3)_2$ and $(ND_3)_2$: $(\theta_A, 180° - \theta_B)$ change from (44°, 66°) to (46°, 64°), experimentally they change from (49°, 65°) to (50°, 63°). So it appears that, even with potential III, $(ND_3)_2$ is more nearly cyclic than $(NH_3)_2$. We can explain this, rather unexpected, observation by analysing the wavefunctions.

When we compare the wavefunction of the lowest G state† of $(ND_3)_2$ in Fig. 4(*b*) with the corresponding wavefunction of $(NH_3)_2$ in Fig. 4(*a*), we clearly observe two effects. First, as expected, the wavefunction of $(ND_3)_2$ has a larger amplitude near the equilibrium position at which it is mainly localized. This leads to an increase of the average dipole moment. Secondly, however, we also observe a substantially larger amplitude of the wavefunction of $(ND_3)_2$ on the side of the other, equivalent, minimum in potential III. This is seen even more clearly in Fig. 5. In order to understand the latter effect one has to remember that, in spite of the equivalence of the two minima in the potential, the G-state wavefunctions are mainly localized on one side because of the *ortho–para* differences. This difference in the behaviour of *ortho* and *para* monomers will be less for ND_3 than for NH_3, because its rotational constant A_z is smaller by a factor of 2. Consequently, the asymmetry in the G-state wavefunctions which is caused by these *ortho–para* differences, will be smaller in $(ND_3)_2$. In other words, $(ND_3)_2$ is more nearly cyclic (in its G state) because of the smaller *ortho–para* differences. This leads to a smaller average dipole moment. Apparently, for potential III with its low interchange barrier of 24 cm^{-1} the latter effect dominates and explains the observed decrease of the dipole moment. The barriers to rotation of the monomers around their C_3 axes are important too, as they determine the amount of localization in ϕ_A and ϕ_B and, thereby, the extent to which the *ortho–para* differences can manifest themselves. The G-state wavefunction of $(ND_3)_2$, when compared with the corresponding wavefunction of $(NH_3)_2$ is indeed more localized‡ in ϕ_A and ϕ_B. For potential I, with its smaller barriers to C_3 rotations, the two effects on the average dipole moment nearly cancel.

† Note that the observed[1,8] dipole moments and nuclear quadrupole splittings all refer to the lowest G state too.

‡ We have checked whether our internal rotor basis, truncated at $j_A^{max} = j_B^{max} = 5$, correctly describes the increased localization in $(ND_3)_2$. To this end, we have performed calculations for the G states with potential III and $j_A^{max} = j_B^{max} = 6$ (total basis size 6024). We had to extend our computer program with an out-of-core diagonalization routine based on the Davidson algorithm.[24] It can be seen in Tables 4 and 6 that the results from these calculations are essentially the same.

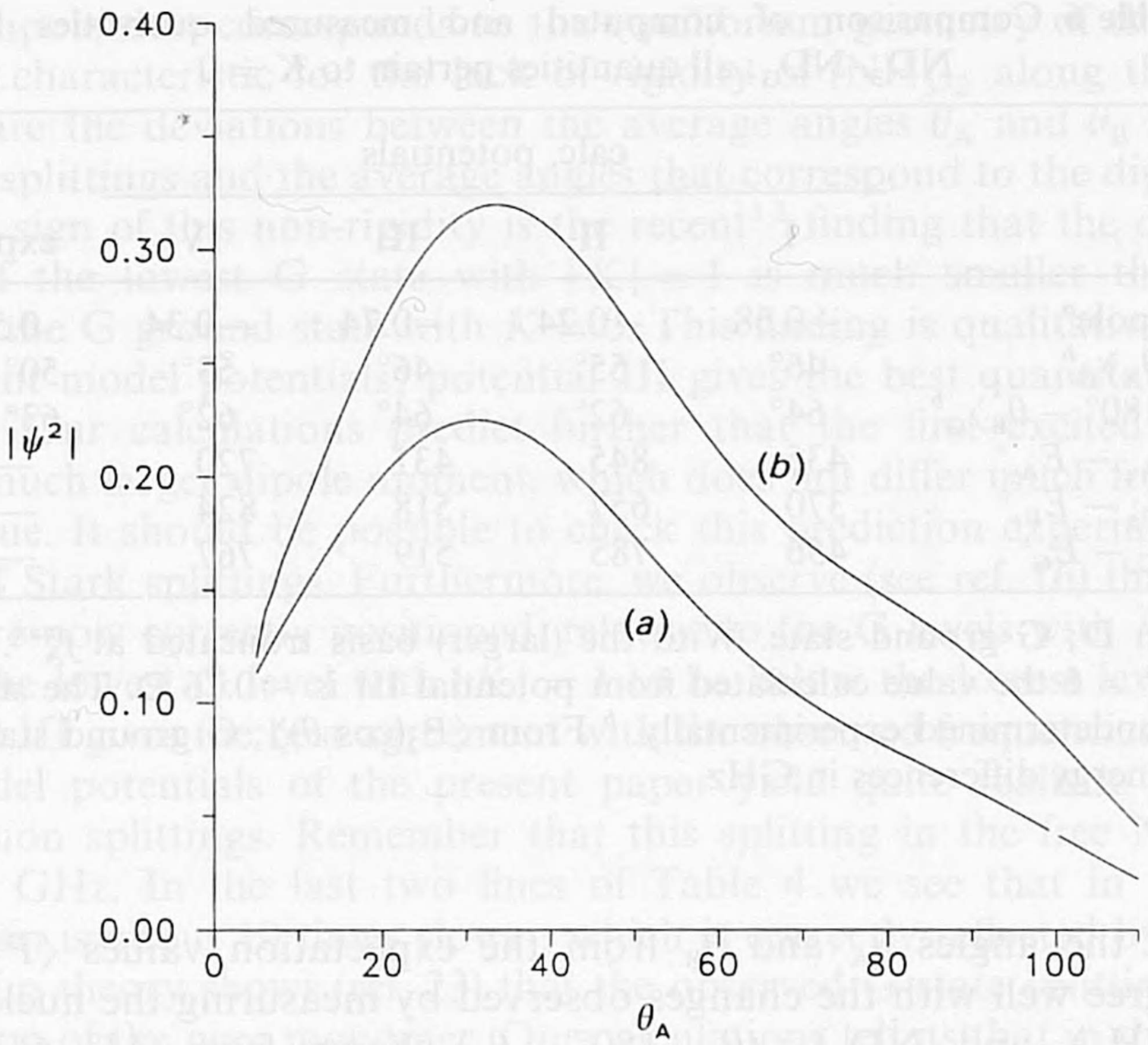

Fig. 5 The G-state wavefunctions of NH_3–NH_3 (*a*) and ND_3–ND_3 (*b*) on the interchange path (*cf.* Fig. 3). Potential used: III.

The isotope shifts in the nuclear quadrupole splittings can be explained by the same two mechanisms which affect the average angles θ_A and θ_B. The increased amplitude of $(ND_3)_2$ on one side of the interchange barrier causes θ_A and θ_B to shift away from the cyclic structure. The decrease in the *ortho–para* difference makes $(ND_3)_2$ more nearly cyclic. The opposite effect of these two mechanisms explains the observation of very small isotope shifts in the nuclear quadrupole splittings. It was these small isotope shifts which led Nelson *et al.*[8] to their conclusion that $(NH_3)_2$ is nearly rigid, and the corresponding decrease of the dipole moment from which they inferred that the equilibrium structure is (nearly) cyclic. In our explanation of these features we do not have to invoke this near-rigidity, nor do we need a nearly cyclic equilibrium structure.

Conclusion

Is the $(NH_3)_2$ riddle solved? Yes, we think it is, in essence, because our calculations have demonstrated that the seemingly contradictory evidence from the various experiments on $(NH_3)_2$ and its isotopomers and from different *ab initio* calculations can be explained by one consistent approach. Our calculations give good agreement with the measured quantities when we use our model potential III, which has a nearly linear hydrogen-bonded equilibrium structure. The interchange barrier in this potential is only about 24 cm^{-1} and this allows large amplitude motions along the interchange path, even for the G (mixed *ortho–para*) states. The fact that this low barrier is caused by a near cancellation of electrostatic and repulsive exchange contributions makes it hard to obtain it accurately from *ab initio* calculations. Remember that the total binding energy amounts to about 1000 cm^{-1}, so that the barrier height is only in the order of 2% of this quantity. Still, as in more rigid hydrogen-bonded complexes, the electrostatic interactions play a dominant role in the binding of $(NH_3)_2$, as they 'prepare' the deep valley in the potential surface in which the interchange between the two equivalent hydrogen-bonded structures takes place. We are now repeating the calculations with the larger angular

basis (with $j_A^{max} = j_B^{max} = 6$), in combination with further improvements in potential III, in order to obtain better quantitative agreement with the experimental data.

We are grateful to Gerrit Groenenboom for his assistance in programming the out-of-core matrix diagonalization algorithm. We thank Rich Saykally and Jenny Loeser (Berkeley), Leo Meerts and Harold Linnartz (Nijmegen), Martina Havenith (Bonn) and Wolfgang Stahl (Kiel) for making available their experimental data before publication and for stimulating discussions.

References

1 D. D. Nelson, G. T. Fraser and W. Klemperer, *J. Chem. Phys.*, 1985, **83**, 6201.
2 S. Liu, C. E. Dykstra, K. Kolenbrander and J. M. Lisy, *J. Chem. Phys.*, 1986, **85**, 2077.
3 M. J. Frisch, J. E. Del Bene, J. S. Binkley and H. F. Schaefer, *J. Chem. Phys.*, 1986, **84**, 2279.
4 K. P. Sagarik, R. Ahlrichs and S. Brode, *Mol. Phys.*, 1986, **57**, 1247.
5 D. M. Hassett, C. J. Marsden and B. J. Smith, *Chem. Phys. Lett.*, 1991, **183**, 449.
6 J. W. I. van Bladel, A. van der Avoird, P. E. S. Wormer and R. J. Saykally, *J. Chem. Phys.*, 1992, **97**, 4750.
7 F-M. Tao and W. Klemperer *J. Chem. Phys.*, 1993, **99**, 5976.
8 D. D. Nelson, W. Klemperer, G. T. Fraser, F. J. Lovas and R. D. Suenram, *J. Chem. Phys.*, 1987, **87**, 6364.
9 D. D. Nelson, G. T. Fraser and W. Klemperer, *Science*, 1987, **238**, 1670.
10 J. G. Loeser, C. A. Schmuttenmaer, R. C. Cohen, M. J. Elrod, D. W. Steyert, R. J. Saykally, R. E. Bumgarner and G. A. Blake, *J. Chem. Phys.*, 1992, **97**, 4727.
11 M. Havenith, R. C. Cohen, K. L. Busarow, D-H. Gwo, Y. T. Lee and R. J. Saykally, *J. Chem. Phys.*, 1991, **94**, 4776.
12 M. Havenith, H. Linnartz, E. Zwart, A. Kips, J. J. ter Meulen and W. L. Meerts, *Chem. Phys. Lett.*, 1992, **193**, 261.
13 H. Linnartz, A. Kips, W. L. Meerts and M. Havenith, *J. Chem. Phys.*, 1993, **99**, 2449.
14 R. M. Baum, *Chem. Eng. News*, 1992, **19**, (October), 20.
15 R. J. Saykally and G. A. Blake, *Science*, 1993, **259**, 1570.
16 E. H. T. Olthof, A. van der Avoird and P. E. S. Wormer, *J. Mol. Struct.* (*Theochem*), 1994.
17 P. E. S. Wormer and H. Hettema, *J. Chem. Phys.*, 1992, **97**, 5592.
18 C. E. Dykstra and L. Andrews, *J. Chem. Phys.*, 1990, **92**, 6043.
19 G. Brocks, A. van der Avoird, B. T. Sutcliffe and J. Tennyson, *Mol. Phys.*, 1983, **50**, 1025.
20 L. Fusina, G. di Lonardo and J. W. C. Johns, *J. Mol. Spectrosc.*, 1985, **112**, 211.
21 J. W. I. van Bladel, A. van der Avoird and P. E. S. Wormer, *J. Phys. Chem.*, 1991, **95**, 5414.
22 D. Papoušek, J. M. R. Stone and V. Špirko, *J. Mol. Spectrosc.*, 1973, **48**, 17.
23 E. H. T. Olthof, A. van der Avoird, P. E. S. Wormer, J. Loeser and R. J. Saykally, manuscript in preparation.
24 E. R. Davidson, *J. Comput. Phys.*, 1975, **17**, 87.

Paper 3/07507I; *Received* 20*th December*, 1993